First Look Murchison Widefield Array observations of Abell 3667

L. Hindson[*A], M. Johnston-Hollitt[A], N. Hurley-Walker[C], J. Morgan[C],K. Buckley[B], E. Carretti[D], K.S. Dwarakanath[E], M. Bell[H,I], G. Bernardi[J], R. Bhat[C], F. Briggs[H,K], A. A. Deshpande[E], A. Ewall-Wice[L], L. Feng[L], B. Hazelton[M], D. Jacobs[F], D. Kaplan[N] N. Kudryavtseva[C], E. Lenc[H,I], B. McKinley[H,K], D. Mitchell[O], B. Pindor[H,P], P. Procopio[H,P], D. Oberoi[G], A. R. Offringa[H,K], S. Ord[C,H], J. Riding[H,P], J. D. Bowman[F], R. Cappallo[Q], B. Corey[Q], D. Emrich[C], B. M. Gaensler[H,I], R. Goeke[Q], L. Greenhill[J], J. Kasper[J], E. Kratzenberg[Q], C. Lonsdale[Q], M. Lynch[C], R. McWhirter[Q], M. Morales[M], E. Morgan[L], T. Prabu[E], A. Rogers[Q], A. Roshi[R], U. Shankar[E], K. Srivani[E], R. Subrahmanyan[E,H], S. Tingay[C,H], M. Waterson[C,K], R. Webster[H,P], A. Whitney[Q], A. Williams[C], C. Williams[L]

Email: Luke.Hindson@vuw.ac.nz

[A] School of Chemical and Physical Sciences, Victoria University of Wellington, Wellington, New Zealand

[B] School of Engineering and Computer Sciences, Victoria University of Wellington, Wellington, New Zealand

[C] ICRAR - Curtin University, Perth, Australia

[D] CSIRO Astronomy and Space Science, PO Box 76, Epping, NSW 1710, Australia

[E] Raman Research Institute, Bangalore, India

[F] School of Earth and Space Exploration, Arizona State University, Tempe, AZ, USA

[G] National Centre for Radio Astrophysics, Pune, India

[H] ARC Centre of Excellence for All-sky Astrophysics (CAASTRO), Redfern, NSW, Australia

[I] Sydney Institute for Astronomy. The University of Sydney, Sydney, Australia

[J] Harvard-Smithsonian Center for Astrophysics, Cambridge, MA, USA

[K] Research School of Astronomy and Astrophysics, The Australian National University, Canberra, Australia

[L] MIT Kavli Institute for Astrophysics and Space Research, Cambridge, MA, USA

[M] Physics Department, University of Washington, Seattle, WA, USA

[N] Physics Department, University of Wisconsin-Milwaukee, Milwaukee, WI, USA

[O] CSIRO Astronomy and Space Science, PO Box 76, Epping, NSW 1710, Australia

[P] School of Physics, The University of Melbourne, Melbourne, Australia

[Q] MIT Haystack Observatory, Westford, MA, USA

[R] National Radio Astronomy Observatory, Charlottesville, WV, USA

Abstract

The Murchison Widefield Array (MWA) is a new low frequency interferometric radio telescope, operating in the remote Murchison Radio Observatory in Western Australia. In this paper we present the first MWA observations of the well known radio relics in Abell 3667 (A3667) between 105 and 226 MHz. We clearly detect the radio relics in A3667 and present flux estimates and spectral indices for these features. The 5-point spectral index of the North-West (NW) relic between 105 and 843 MHz varies from -1.17 to -1.41 and is consistent with results found at higher frequencies.

1. INTRODUCTION

Observations of galaxy clusters in the radio regime have revealed low surface brightness and large-scale non-thermal emission up to Mpc-scales associated with some galaxy clusters. These radio sources are known as radio halos and relics and share some observational properties: they have steep synchrotron spectra ($\alpha \sim -1.2$ to -1.4) and are characterised by low surface brightness emission ($\sim \mu$Jy arcsec^{-2}). Radio halos are unpolarised and located towards the centre of the host galaxy cluster, whilst relics are highly polarised and reside on the periphery of the galaxy cluster.

The galaxy cluster A3667 is one of the most well studied examples of radio relic emission in the southern sky. The dramatic radio relics on the periphery of the cluster are believed to be generated by shocks in the intra cluster medium generated by two merging clusters. With an angular extent of $\sim 1°$ and redshift of z=0.0556 (distance of 224 Mpc), A3667 extends over ~ 4 Mpc.

The MWA is one of the Square Kilometre Array precursor telescopes at low frequencies, operating in the regime between 80 and 300 MHz. Details of the technical design and specifications of the MWA can be found in [1] and a review of the scientific goals are presented in [2]. The unifying design theme of the MWA emphasises high survey efficiency and surface brightness sensitivity at low frequency. This makes it an ideal instrument with which to carry out large scale untargeted

Frequency (MHz)	FOV degrees (°)	Resolution arc minutes (′)	Sensitivity (mJy beam^{-1})
120.335	15.9	5.3×3.8	45.3
149.135	13.2	4.2×3.0	31.2
179.855	11.2	3.6×2.5	33.0
225.935	9.8	3.0×2.1	14.2

surveys in search for diffuse, steep-spectrum synchrotron emission associated with radio halos and relics.

In this paper we present the first MWA observations of A3667 between 105.335 to 225.935 MHz. In section 2 we present the observations and briefly outline the data reduction process. In section 3 we present the results of these observations including images of the radio data, integrated fluxes of emission features and a spectral index map of A3667.

2.   OBSERVATIONS & DATA REDUCTION PROCEDURES

A3667 was observed using 114 tiles of the full 128 tile MWA array. The observations consist of 3×232 s "snapshots" of four 30.72 MHz wide bands centred on 120.335, 149.135, 179.855 and 210.575 MHz. The minimum and maximum baselines were 7.7 and 2864 m respectively. This provides sensitivity to structures from $\sim 3'$ to several degrees. The combined uv coverage of three snapshots at 149.135 MHz, excluding multi frequency synthesis (MFS), can be seen in Fig .1. The uv coverage at short baselines provides excellent sensitivity to large scale structure, however the low frequency relative to the maximum baseline limits the resolution to $\sim 3'$.

The data were processed using both pre-existing and bespoke software written specifically for MWA processing. The pre-processing pipeline COTTER was used to perform initial detection and flagging of radio frequency interference using AOFLAGGER [3] and data averaging to 1 s and 40 kHz time and frequency resolution. Gain solutions were determined by using the BANDPASS task in CASA on a pointed observation of 3C444. Imaging was carried out using standard MIRIAD routines. A robust weighting

Fig. 1.   **Combined uv coverage for 3×232 snapshots centred on 149.135 MHz with a bandwidth of 30.72 MHz, in units of wavelength. Due to the large data set size we only show a single frequency channel. Including MFS fills most of the uv plane.**

scheme of 0.0 was used to provide a good compromise between the high sensitivity provided by natural weighting while almost maintaining the synthesised beam of uniform weighting. The observing properties including sensitivity are summarised in table .I. Full details of the data reduction, imaging and flux calibration will be presented in [4].
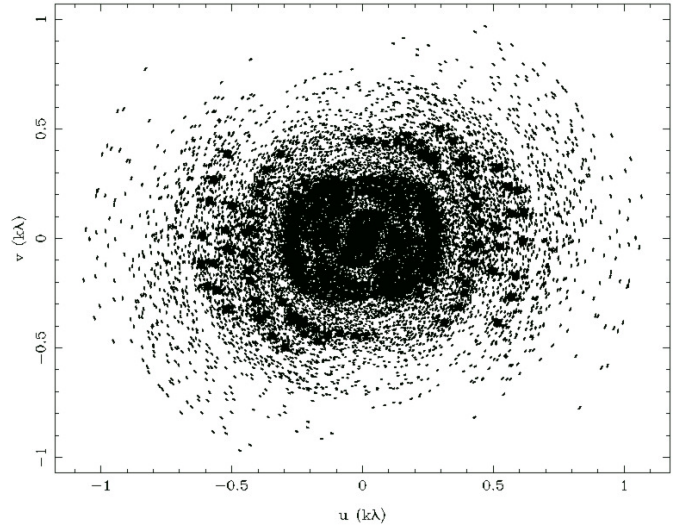
3.   RESULTS

In the top panel of Fig .2 we present the entire field of view (FOV) of our 120.335 MHz image centred on A3667. This image highlights the incredibly wide FOV that makes the MWA an excellent survey instrument. We present a zoomed in image of the 225.935 MHz band in Fig .3 with contours taken from re-reduced Molonglo data [5] at 843 MHz.

These observations clearly detect the NW and South-East (SE) relics on the periphery of the cluster. The peak brightness of the NW and SE relics is 4.6 and 1.5 Jy/beam at 149.135 MHz respectively. At 120.335 MHz we find that the SE relic becomes blended with sources labelled A and B. Towards the centre of the cluster we identify the bright head-tail radio galaxy B2007-569 which has a peak brightness of 5.4 Jy/beam at 149.135 MHz. We also highlight the radio galaxy PKS2014-55 which exhibits an interesting cross shaped morphology.
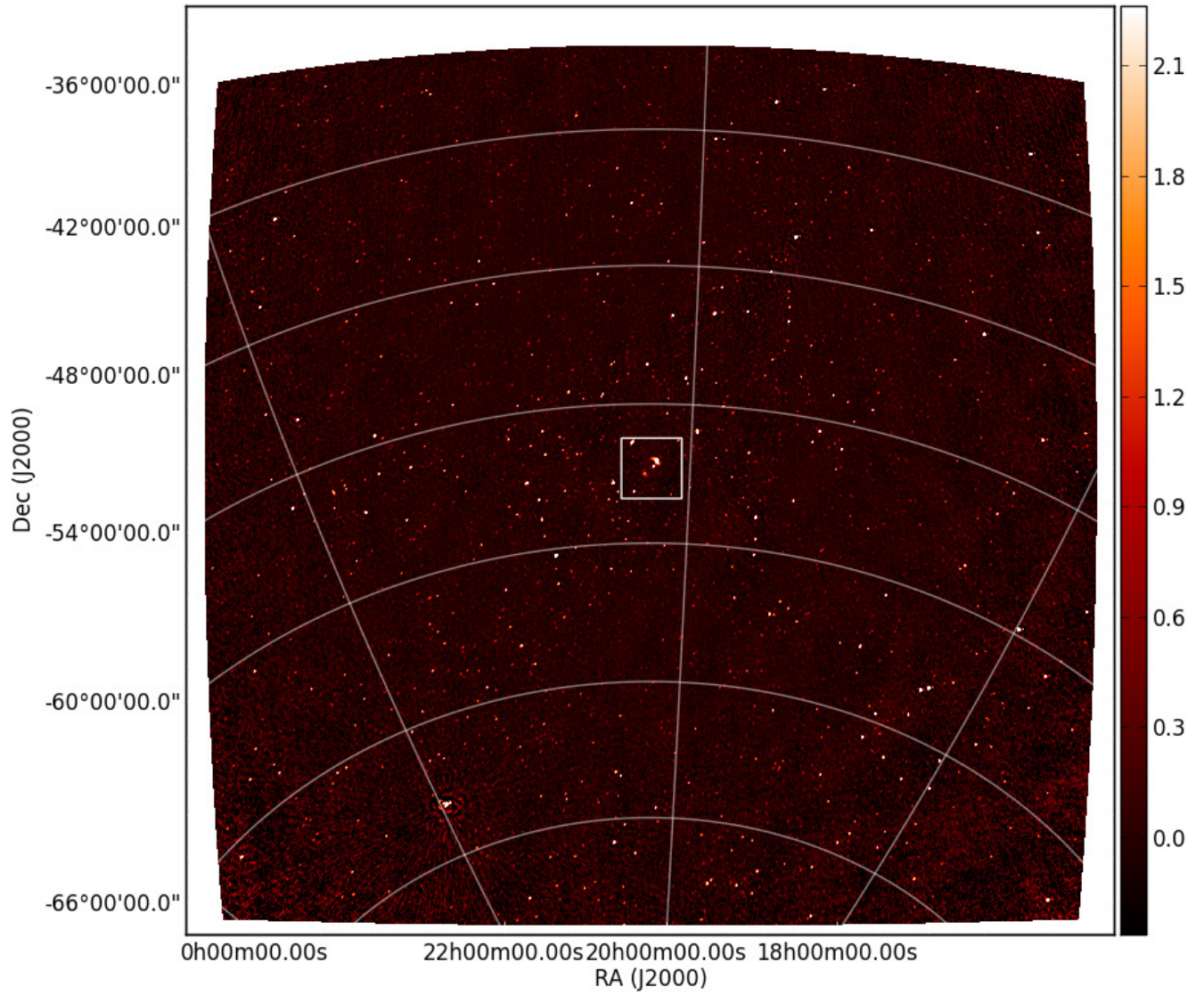
Fig. 2. **Top panel: full field of view of the primary beam and flux corrected 120.335 MHz image. The white box highlights the region we show in Fig .3.**
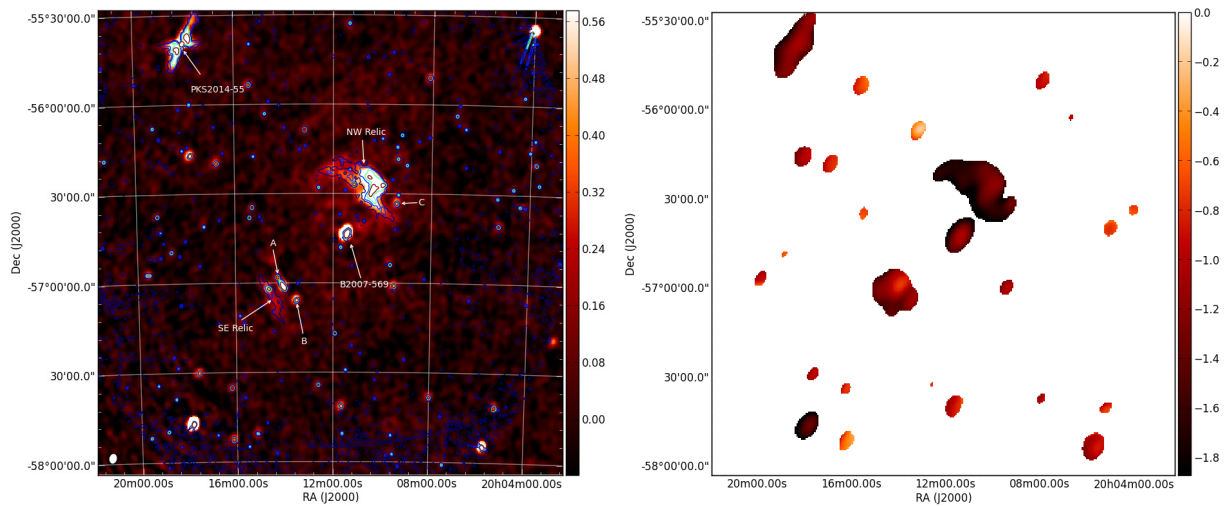

Fig. 3. **Left panel: zoomed in image of A3667 at 225.935 MHz. The synthesised beam is shown in the bottom left and contours show 843 MHz data. Right panel: Spectral index map of A3667 from 120.335 to 843 MHz.**

4. Integrated Fluxes and Spectral Indices

We determine the integrated flux of the relics in A3667 by fitting apertures around the sources above 3σ. The integrated flux at 149.135 MHz for the NW and SE relics is 42.8 and 3.7 Jy respectively. To explore the spectral properties of the two relics we first fit the four point spectral index using a power law and find a spectral index between 120.335 and 225.935 MHz of -1.13 ± 0.28.

We generate spectral index maps of A3667 by first convolving our MWA band images and Molonglo data with a common Gaussian kernel slightly larger than the beam at 120.335 MHz. We then fit a power-law to each pixel above $3\sigma_{\mathrm{rms}}$. The resultant spectral index map can be seen in the right panel of Fig .3. The spectral index of the NW relic is fairly steep at -1.41 ± 0.36 and varies from -1.17 towards to centre to -2.29 on the inner periphery. These results are consistent with the 3-point spectral index values between 843 MHz and 2.4 GHz (Johnston-Hollitt, 2003). The spectral index of the SE relic is blended with sources A and B. However, using just the higher frequency observations will allow us to more accurately determine the spectral index of this relic.

Fig. 4. **T-T plot of the NW relic between 225.935 to 843 MHz with the best fit to the data, spectral index and chi-squared value.**

We are able to generate a T-T plot of the large NW relic between 225.935 and 843 MHz. We convolve the 843 MHz map with a Gaussian equal to the 225.935 MHz beam and then regrid both maps so a single pixel corresponds to the size of the beam. Plotting the pixel flux at 843 MHz against the corresponding flux at 225.935 MHz in these maps and fitting a straight line results in an average spectral index for the NW relic of -1.33 ± 0.07 (Fig .4). This technique accounts for the possibility of constant offsets between maps due to missing short spacings or large-scale foreground contamination.
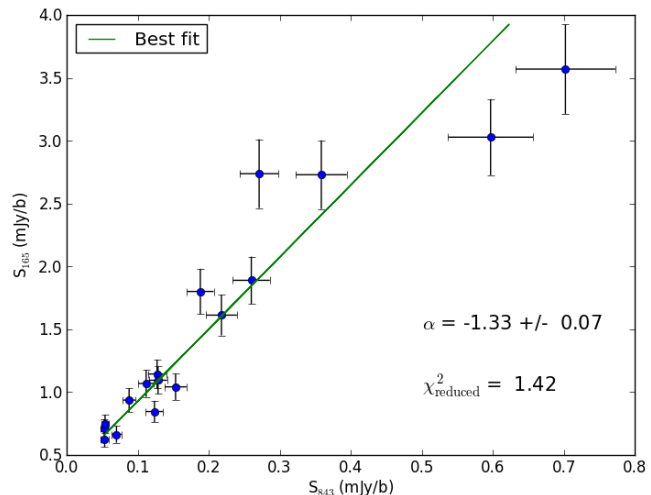
5. Acknowledgements

References

[1] S. J. Tingay, R. Goeke, J. D. Bowman, D. Emrich, S. M. Ord, D. A. Mitchell, M. F. Morales, T. Booler, B. Crosse, R. B. Wayth, C. J. Lonsdale, and et al., "The Murchison Widefield Array: The Square Kilometre Array Precursor at Low Radio Frequencies," *PASA*, **vol. 30**, p. 7, Jan. 2013.

[2] J. D. Bowman, I. Cairns, D. L. Kaplan, T. Murphy, D. Oberoi, L. Staveley-Smith, W. Arcus, D. G. Barnes, G. Bernardi, F. H. Briggs, S. Brown, J. D. Bunton, and et al., "Science with the Murchison Widefield Array," *PASA*, **vol. 30**, p. 31, Apr. 2013.

[3] A. R Offringa, J. J. van de Gronde, and J. B. T. M. Roerdink, "A morphological algorithm for improving radio-frequency interference detection," *A&A*, **vol. 539**, p. A95, Mar. 2012.

[4] L. Hindson, M. Johnston-Hollitt, N. Hurley-Walker, and et al., "First MWA observations of cluster scale non-thermal emission: the case of A3667," *MNRAS*, **in prep**. 2014

[5] M. Johnston-Hollitt, "Detection of magnetic fields and diffuse radio emission in Abell 3667 and other rich southern clusters of galaxies," *Ph.D. dissertation*, University of Adelaide, Jul. 2003.